

MOL (011676)

The effects of subunit composition on the inhibition of nicotinic receptors by the amphipathic blocker TMPH

Roger L. Papke, Joshua D. Buhr, Michael M. Francis, Kyung Il Choi, Jeffrey S. Thinschmidt, and Nicole A. Horenstein

Department of Pharmacology and Therapeutics; RLP, JDB, MMF, JST
University of Florida, College of Medicine
Gainesville, FL 32610

Department of Chemistry; KIC, NAH
University of Florida
Gainesville, FL 32610

Present address, MMF: University of Utah
Department of Biology
Salt Lake City Utah 84112

Present address, KIC: Korea Institute of Science and Technology
39-1 Hawolgok-dong, Seongbuk-gu,
Seoul, 136-791, Korea

MOL (011676)

Selective inhibition of nAChR

Running title: Selective inhibition of nAChR

Corresponding author:

Roger L. Papke Ph.D.
Associate Professor of Pharmacology and Therapeutics
100267 JHMHSC, 1600 SW Archer Rd.
University of Florida, College of Medicine
Gainesville, FL 32610
USA

Phone: 352-392-4712

Fax: 352-392-9696

rlpapke@ufl.edu

Number of text pages	16
Number of tables	2
Number of figures	11
Number of references	19
Number of words in the Abstract	183
Number of words in the Introduction	388
Number of words in the Discussion	689

non-standard abbreviations

TMPH 2,2,6,6-tetramethylpiperidin-4-yl heptanoate

BTMPS bis-(2,2,6,6-tetramethyl-4-piperidiny)-sebacate

Abstract

The therapeutic targeting of nicotinic receptors in the brain will benefit from the identification of drugs which may be selective for their ability to activate or inhibit a limited range of nicotine acetylcholine receptor subtypes. In the present study we describe the effects of 2,2,6,6-tetramethylpiperidin-4-yl heptanoate (TMPH), a novel compound that is a potent inhibitor of neuronal nicotinic receptors. Evaluation of nAChR subunits expressed in *Xenopus* oocytes indicated that TMPH can produce a potent and long-lasting inhibition of neuronal nAChR formed by the pairwise combination of the most abundant neuronal alpha (i.e. $\alpha 3$ and $\alpha 4$) and beta subunits ($\beta 2$ and $\beta 4$), with relatively little effect, due to rapid reversibility of inhibition, on muscle-type ($\alpha 1\beta 1\gamma\delta$) or $\alpha 7$ receptors. However, the inhibition of neuronal beta subunit-containing receptors was also decreased if any of the nonessential subunits $\alpha 5$, $\alpha 6$, or $\beta 3$ were coexpressed. This decrease in inhibition is shown to be associated with a single amino acid present in the second transmembrane domain of these subunits. Our data indicate a great potential utility for TMPH to help relate the diverse CNS effects to specific nAChR subtypes.

Introduction

There are multiple types of nicotine acetylcholine receptors (nAChR) in the brain associated with synaptic function, signal processing or cell survival. The therapeutic targeting of nicotinic receptors in the brain will benefit from the identification of drugs which may be selective for their ability to activate or inhibit a limited range of these receptor subtypes. Mecamylamine is a ganglionic blocker developed many years ago as an antihypertensive and more recently suggested to be useful as a component in the pharmacotherapy for Tourette's syndrome (Sanberg et al., 1998) and smoking cessation (Rose et al., 1994). However, electrophysiological characterization of mecamylamine has shown it to be relatively nonselective (Papke et al., 2001), consistent with the observation that it effectively blocks all of the peripheral and central nervous system (CNS) effects of nicotine (Martin et al., 1993). We previously identified a family of bis-tetramethylpiperidine compounds as inhibitors of neuronal type nicotinic receptors (Francis et al., 1998). The prototype compound in this series is BTMPS (bis-(2,2,6,6-tetramethyl-4-piperidiny)-sebacate), which produces a readily reversible block of muscle-type nAChR and a nearly irreversible use-dependent, voltage-independent block of neuronal nAChR. The tetramethyl-piperidine groups of BTMPS are sufficient to produce block of nAChR, and the conjugation of two such groups with a long aliphatic chain accounts for both the selectivity and slow reversibility of BTMPS inhibition of neuronal nAChR (Francis et al., 1998). In the present study we describe the effects of 2,2,6,6-tetramethylpiperidin-4-yl heptanoate (TMPH), a novel compound that has a single tetramethyl-piperidine group and an aliphatic chain similar to that of BTMPS. TMPH is also a potent inhibitor of neuronal nicotinic receptors.

Simple models for nAChR subtypes are provided by pairwise combinations of alpha and beta subunits expressed in *Xenopus* oocytes. However, there is a growing appreciation that ancillary subunits such as $\alpha 5$, $\alpha 6$ and $\beta 3$, that work poorly in pairwise combinations with other single subunits, nonetheless contribute to functionally important receptor subtypes in vivo. We show that for the commonly used nAChR subunit pairwise combinations inhibition by TMPH is

only very slowly reversible. However, the incorporation of these additional subunits results in receptors that recover more rapidly and would thus show lower equilibrium inhibition *in vivo*. Therefore, based on the characterization of this agent's effects on specific nAChR subtypes, TMPH may identify the particular molecular substrates that underlie the multiple effects of nicotine in the brain.

Methods

Synthesis.

Chemicals used for the synthesis were purchased from Aldrich Chemical Company. Compounds were characterized by ¹H-NMR and FAB-MS.

TMPH synthesis

To a mixture of 2,2,6,6-tetramethyl-4-piperidinol (472 mg, 3.0 mmol) and methyl heptanoate (476 mg, 3.3 mmol) in 3.0 mL of dimethyl formamide was added 250 mg of powdered potassium carbonate. The resulting mixture was heated at 145~155 °C for 64 h under a gentle stream of N₂. After cooling, the reaction mixture was partitioned between water and hexanes. The organic layer was separated, washed with water (2x) and brine, then dried over anhydrous MgSO₄ and evaporated to afford the crude product as an oil. The oil was dissolved in MeOH and was then treated with 2 equivalents of conc. HCl. The solvent was removed *in vacuo*, and the residue was then treated with diethyl ether. The resulting solids were removed by filtration. The ethereal filtrate was concentrated *in vacuo* and triturated with hexane to afford 380 mg (41%) of TMPH hydrochloride. It was recrystallized from boiling ethyl acetate/hexane to afford short colorless needles, mp 113 - 115 °C. FAB-HRMS: calculated(C₁₆H₃₂NO₂): 270.2433 found: 270.2435

Expression in *Xenopus* oocytes

Mature (>9 cm) female *Xenopus laevis* African frogs (Nasco, Ft. Atkinson, WI) were used as a source of oocytes. Prior to surgery, frogs were anesthetized by placing the animal in a 1.5 g/l solution of MS222 (3-aminobenzoic acid ethyl ester) for 30 min. Oocytes were removed from an incision made in the abdomen.

In order to remove the follicular cell layer, harvested oocytes were treated with 1.25 mg/ml Type 1 collagenase (Worthington Biochemical Corporation, Freehold, NJ) for 2 hours at room temperature in calcium-free Barth's solution (88 mM NaCl, 1 mM KCl, 0.33 mM MgSO₄, 2.4 mM NaHCO₃, 10 mM HEPES (pH 7.6), 50 mg/l gentamicin sulfate). Subsequently, stage 5 oocytes were isolated and injected with 50 nl (5-20 ng) each of the appropriate subunit cRNAs. Recordings were made 2 to 15 days after injection.

Preparation of RNA

Rat neuronal nAChR clones and mouse muscle nAChR cDNA clones were used. The wild-type clones were obtained from Dr. Jim Boulter (UCLA). The rat $\alpha 6/3$ (Dowell et al., 2003) clone was obtained from Michael McIntosh (University of Utah) and expressed in *Xenopus* oocytes in combinations with rat $\beta 2$ and $\beta 3$. The original $\alpha 6/3$ construct provided was sequenced and was found to have a mutation in the second transmembrane domain (TM2) sequence which exchanged a valine for an alanine in the 7' position (TM2 numbering scheme (Miller, 1989)). The TM2 domain is understood to line the pore of the channel, with alpha helix structure. The 7' position may actually be directed away from the actual pore lining, but this residue is highly conserved in all of the nAChR. It is valine in all of them except $\alpha 9$ (isoleucine) and $\beta 1$, where it is alanine. The TM2 mutation in the $\alpha 6/3$ chimera was corrected by using QuickChange (Stratagene) according to their protocols. The corrected $\alpha 6/3$ chimera sequence was confirmed by restriction diagnostics and automated fluorescent sequencing (University of Florida core facility). The corrected clone was expressed as above in *Xenopus* oocytes with $\beta 2$ and $\beta 3$ and compared to the wild-type $\alpha 3$ co-expressed with $\beta 2$ and $\beta 3$.

After linearization and purification of cloned cDNAs, RNA transcripts were prepared *in vitro* using the appropriate mMessage mMachine kit from Ambion Inc. (Austin, TX).

Electrophysiology

The majority of experiments were conducted using OpusXpress 6000A (Axon Instruments, Union City California). OpusXpress is an integrated system that provides automated impalement and voltage clamp of up to eight oocytes in parallel. Cells were automatically perfused with bath

solution, and agonist solutions were delivered from a 96-well plate. Both the voltage and current electrodes were filled with 3 M KCl. The agonist solutions were applied via disposable tips, which eliminated any possibility of cross-contamination. Drug applications alternated between ACh controls and experimental applications. Flow rates were set at 2 ml/min for experiments with $\alpha 7$ receptors and 4 ml/min for other subtypes. Cells were voltage-clamped at a holding potential of -60 mV. Data were collected at 50 Hz and filtered at 20 Hz. Agonist applications were 12 s in duration followed by 181 s washout periods for $\alpha 7$ receptors and 8 s with 241 s wash periods for other subtypes. For some experiments, particularly under conditions where residual inhibition precluded making repeated measurements from single cells (see below), manual oocyte recordings were made as previously described (Papke and Papke, 2002). In brief, Warner Instruments (Hamden, CT) OC-725C oocyte amplifiers were used, and data were acquired with a minidigi or digidata 1200A with pClamp9 software (Axon Instruments). Sampling rates were between 10 and 20 Hz and the data were filtered at 6 Hz. Cells were voltage clamped at a holding potential of -50 mV. Data obtained with these methods were comparable to those obtained with OpusXpress.

Experimental protocols and data analysis

Each oocyte received two initial control applications of ACh, an experimental drug application (or co-application of ACh and TMPH), and then follow-up control application(s) of ACh. The control ACh concentrations for $\alpha 1\beta 1\gamma\delta$, $\alpha 3\beta 4$, $\alpha 4\beta 2$, $\alpha 3\beta 2$, $\alpha 3\beta 2\alpha 5$, $\alpha 3\beta 2\beta 3$, $\alpha 6/3\beta 2\beta 3$, $\alpha 6\beta 4\beta 3$ and $\alpha 7$, receptors were $\bar{\square}$ μM , 100 μM , 10 μM , 30 μM , 1 μM , 100 μM , 100 μM , 100 μM , and 300 μM , respectively. These concentrations were selected since they gave large responses with relatively little desensitization so that the same oocyte could be stimulated repeatedly with little decline in the amplitude of the ACh responses. This allowed us to separate out the inhibitory effects of the antagonist from possible cumulative desensitization.

Responses to experimental drug applications were calculated relative to the preceding ACh control responses in order to normalize the data, compensating for the varying levels of channel expression among the oocytes. Responses were characterized based on both their peak

amplitudes and the net charge (Papke and Papke, 2002). In brief, for net charge measurement a 90-second segment of data beginning 2 s prior to drug application was analyzed from each response. Data were first adjusted to account for any baseline offset by subtracting the average value of 5 s period of baseline prior to drug application from all succeeding data points. When necessary, baseline reference was also corrected for drift using Clampfit 9.0 (Axon Instruments, Union City CA). Following baseline correction, net charge was then calculated by taking the sum of all the adjusted points. The normalized net charge values were calculated by dividing the net charge value of the experimental response by the net charge value calculated for the preceding ACh control response. Means and standard errors (SEM) were calculated from the normalized responses of at least 4 oocytes for each experimental concentration. In order to measure the residual inhibitory effects, this subsequent control response was compared to the pre-application control ACh response.

For concentration-response relations, data derived from net charge analyses were plotted using Kaleidagraph 3.0.2 (Abelbeck Software; Reading, PA), and curves were generated from the Hill equation

$$\text{Response} = \frac{I_{\max} [\text{agonist}]^n}{[\text{agonist}]^n + (EC_{50})^n}$$

where I_{\max} denotes the maximal response for a particular agonist/subunit combination, and n represents the Hill coefficient. I_{\max} , n , and the EC_{50} were all unconstrained for the fitting procedures. Negative Hill slopes were applied for the calculation of IC_{50} values.

Brain slice recording

Male Sprague Dawley rats (p11-p20) were anesthetized with Halothane (Halocarbon Laboratories, River Edge, NJ) and swiftly decapitated. Transverse (300mm) whole brain slices were prepared using a vibratome and a high Mg^{+} /low Ca^{2+} ice-cold artificial cerebral spinal fluid (ACSF) containing (in mM) 124 NaCl, 2.5 KCL, 1.2 NaH_2PO_4 , 2.5 $MgSO_4$, 10 D-glucose, 1 $CaCl_2$, and 25.9 $NaHCO_3$ saturated with 95% O_2 -5% CO_2 . Slices were incubated at 30°C for 30 minutes and then left at room temperature until they were transferred to a submersion

chamber for recording. During experiments slices were perfused (2ml/min) with normal ACSF containing (in mM) 126 NaCl, 3 KCL, 1.2 NaH₂PO₄, 1.5 MgSO₄, 11 D-glucose, 2.4 CaCl₂, 25.9 NaHCO₃, and 0.008 atropine sulfate saturated with 95% O₂-5%CO₂ at 30°C. Medial septum/diagonal band cells were visualized with infrared differential interference contrast microscopy using a Nikon E600FN microscope. Whole cell patch-clamp recordings were made with glass pipettes (3-5MΩ) containing an internal solution of (in mM) 125 K-gluconate, 1 KCL, 0.1 CaCl₂, 2 MgCl₂, 1 EGTA, 2 MgATP, 0.3 Na₃GTP, and 10 HEPES. Cells were held at -70mV, and a -10mV/10ms test pulse was used to determine series and input resistances. Cells with series resistances > 60 MΩ or those requiring holding currents > 200pA were not included in the final analyses. Local somatic application of 1mM ACh and 1mM ACh + 300μM TMPH was performed using double barrel glass pipettes attached to a picospritzer (General Valve, Fairfield, NJ) with Teflon tubing (10-20psi for 5ms-30ms). For each cell two baseline evoked responses to ACh were recorded followed by two evoked responses to ACh + TMPH (interstimulus interval of 30 sec). ACh was then applied every 30 seconds for the remainder of the experiment. Signals were digitized using an Axon digidata 1200A and sampled at 20kHz using Clampex version 9. Data analysis was done with Clampfit version 9.

Results

TMPH inhibition of AChR subtypes

TMPH (Figure 1) was initially tested on mouse muscle-type ($\alpha 1\beta 1\epsilon\delta$) nAChR, three different pairwise combinations of rat neuronal alpha and beta subunits ($\alpha 3\beta 4$, $\alpha 4\beta 2$, and $\alpha 3\beta 2$), and $\alpha 7$ homomeric neuronal nAChR. Additionally combinations of three subunits and an $\alpha 6/3$ chimera were also tested. The results are summarized in Table 1. As shown in Figure 1, both muscle-type and $\alpha 3\beta 4$ receptors (a minimal model for ganglionic-type receptors) were inhibited during the co-application of ACh and TMPH. However, while the inhibition of muscle-type receptors was readily reversible after a 5 minute wash, the inhibition of $\alpha 3\beta 4$ receptors persisted after the wash. The data also indicate that the inhibition of $\alpha 3\beta 4$ receptors became progressively

greater during the co-application response so that the inhibition of net charge was greater than the inhibition of peak current. This was not the case for the inhibition of muscle-type receptors. The other neuronal alpha-beta subunit pairs tested, $\alpha 4\beta 2$ and $\alpha 3\beta 2$, were blocked in a fashion similar to $\alpha 3\beta 4$ receptors (Figure 2), with a larger inhibition of net charge than peak current and virtually no recovery following a 5 minute wash. In contrast, $\alpha 7$ receptors, like muscle-type receptors, showed little difference between the inhibition of peak currents and net charge and showed significant recovery after a 5 minute wash (Figure 2). These differences are reflected in the IC_{50} values presented in Table 1. Note that receptors which rapidly equilibrate inhibition and recover readily (e.g. muscle-type receptors and $\alpha 7$) have ratios of the IC_{50} for net charge to the IC_{50} for peak currents of close to 1 (Table 2). In contrast, for receptor types which show progressively more inhibition during the co-application and have slow recovery, the ratio of the IC_{50} for net charge to the IC_{50} for peak currents is much less than 1. Consequently, for receptors which show progressively more inhibition during the co-application IC_{50} values estimated from the inhibition of net charge are similar to those which can be derived from persistent inhibition measured after a 5 minute wash (i.e. from the recovery data, see Table 2).

Neuronal nAChR recovery rates

Our initial experiments evaluated recovery after only a single 5 minute wash. In order to evaluate the actual rates at which $\alpha 7$ and the various nAChR pairwise subunit combinations recovered from TMPH-induced inhibition, we made repeated applications of ACh alone after a single co-application of ACh and TMPH. As shown in Figure 3, the rat $\alpha 4\beta 2$, $\alpha 3\beta 2$, $\alpha 3\beta 4$ receptors showed virtually no detectable recovery over a period of 30 minutes, while $\alpha 7$ receptors were fully recovered after about 15 minutes of wash.

Use-dependence of inhibition by TMPH

We evaluated the degree to which inhibition by TMPH was use-dependent by applying 1 μM TMPH alone and comparing the response to a subsequent control ACh application to that obtained after 1 μM TMPH was co-applied with ACh. As shown in Figure 4, the ability of TMPH to inhibit neuronal nAChR when applied in the absence of agonist varied significantly

among the pairwise subunit combinations tested, but in all cases was less than when TMPH was co-applied with agonist. Interestingly, while TMPH alone applied to $\alpha 4\beta 2$ receptors was almost as effective as when co-applied with ACh, TMPH alone applied to $\alpha 3\beta 2$ receptors had no detectable effect after the washout period.

Progressive inhibition of $\alpha 4\beta 2$ receptors by repeated co-applications of ACh and TMPH below its IC_{50} value

The IC_{50} values presented in Table 1 were based on the inhibition produced by single co-applications (20 seconds in duration) of ACh and TMPH. Since for the neuronal beta subunit-containing receptors the onset of inhibition is apparently much faster than the reversibility of inhibition, measurements based on single applications of TMPH are likely to underestimate what equilibrium IC_{50} s would be. In order to test the hypothesis that repeated applications of TMPH would produce an accumulated inhibition that would be greater than the inhibition produced by a single application, we made repeated co-applications of ACh and 100 nM TMPH to oocytes expressing $\alpha 4\beta 2$ receptors. Co-applications of TMPH and ACh were alternated with applications of ACh alone. As shown in Figure 5, repeated co-applications of ACh with 100 nM TMPH (the IC_{50} in single-dose experiments) produced 90% inhibition after 3 applications at 10 minute intervals. Further applications did not produce additional inhibition. Making a corresponding shift in the $\alpha 4\beta 2$ net charge inhibition curve in Figure 3 (i.e. so that 100 nM is the IC_{90} rather than the IC_{50}) suggests that the equilibrium IC_{50} would be approximately 10 nM.

The effect of $\alpha 5$ co-expression with $\alpha 3\beta 2$ subunits on the sensitivity to TMPH

As noted above, efforts to connect data obtained from oocyte studies with *in vivo* data can be complicated by the fact that nAChR *in vivo* may have more complex subunit composition than the simple pairwise alpha/beta subunit combinations most readily tested in oocytes. One such subunit that contributes to the complexity of AChRs *in vivo* is $\alpha 5$, which is not required to co-assemble with other subunits in order for them to function but is likely to be present in some receptor subtypes *in vivo* (Gerzanich et al., 1998; Wang et al., 1996). We tested the hypothesis that the presence of the $\alpha 5$ subunit could modulate the sensitivity of a neuronal nAChR subunit

to TMPH. For these experiments we used human $\alpha 3$ and $\beta 2$ subunits, which readily form receptors with or without the co-expression of the human $\alpha 5$ subunit. We chose to use these subunits since the successful inclusion of the $\alpha 5$ subunit produces an easily detectable change in receptor pharmacology, increasing the potency of ACh (Gerzanich et al., 1998). All batches of oocytes used for these experiments were confirmed to have this predicted effect of $\alpha 5$ expression.

As shown in Figure 6, ACh responses of oocytes expressing human $\alpha 3\beta 2$ and human $\alpha 3\beta 2\alpha 5$ showed similar sensitivity to TMPH during the initial co-application. (The IC_{50} values based on net charge analysis were 460 ± 170 nM and 430 ± 180 nM, respectively.) However, as shown in Figure 7, oocytes expressing $\alpha 5$ along with $\alpha 3$ and $\beta 2$ showed much faster recovery than those expressing $\alpha 3$ and $\beta 2$ alone. The responses of oocytes expressing $\alpha 3\beta 2\alpha 5$ had a half time of recovery of about 15 minutes, while those expressing human $\alpha 3\beta 2$ receptors showed no significant recovery over a period of 40 minutes, similar to the oocytes expressing rat $\alpha 3\beta 2$ receptors (Figure 3).

Inhibition of receptors containing $\beta 3$ and $\alpha 6$ subunits.

It has been suggested that *in vivo* $\beta 3$ subunits may co-assemble with $\alpha 6$ and possibly $\alpha 4$ and $\beta 2$ to make receptors that regulate dopamine release (Champiaux et al., 2003). However, the $\alpha 6$ subunit expresses poorly in oocytes when used in pairwise combinations with beta subunits (Kuryatov et al., 2000). One approach to get around this problem has been to use a chimera of $\alpha 6$ and $\alpha 3$ which has improved expression properties. Due to the presence of the $\alpha 6$ extracellular domain, receptors formed with this chimera are sensitive to $\alpha 6$ -selective competitive antagonists (Dowell et al., 2003). We compared the effects of TMPH on oocytes expressing $\alpha 3\beta 2\beta 3$ and a chimera of $\alpha 6$ and $\alpha 3$ subunits, $\alpha 6/3$ (Dowell et al., 2003) along with $\beta 2$ and $\beta 3$. This approach allowed us to systematically evaluate first the effects of the $\beta 3$ subunits (by comparing oocytes injected with $\alpha 3\beta 2\beta 3$ to those expressing $\alpha 3\beta 2$ alone) and second the effects of the $\alpha 6$ extracellular domain (by comparing $\alpha 6/3\beta 2\beta 3$ to $\alpha 3\beta 2\beta 3$).

The addition of the $\beta 3$ subunit to the $\alpha 3$ and $\beta 2$ subunits, had the effect of decreasing sensitivity to an initial application of TMPH (Figure 8A), such that the IC_{50} for inhibiting $\alpha 3\beta 2\beta 3$ receptors was at least an order of magnitude higher than for the inhibition of $\alpha 3\beta 2$ without $\beta 3$ (Figures 2 and 8, see also Table 1). The receptors containing the $\alpha 6/3$ chimera in combination with $\beta 2$ and $\beta 3$ were not significantly different in their sensitivity to TMPH from those made up of the $\alpha 3\beta 2\beta 3$ wild-type subunits (Figure 8B and Table 1). The recovery of $\beta 3$ -containing receptors from TMPH was relatively complex. There was about 50% recovery in the first 10 minutes, but no further recovery after that. This was similar for both $\alpha 3\beta 2\beta 3$ and $\alpha 6/3\beta 2\beta 3$ (Figure 8C). One possible explanation for this would be if the co-expression of these subunits resulted in mixed populations of receptors, some containing $\beta 3$ subunits and showing rapid recovery, and others formed without $\beta 3$ and showing the nearly irreversible block seen when $\alpha 3$ and $\beta 2$ are expressed as a pair. This is certainly a likely scenario for the combination containing wild-type $\alpha 3$, and may also be the case for the combination containing the chimera, since in our experience there is about a two-fold increase in currents when $\beta 3$ is co-expressed with $\beta 2$ and the $\alpha 6/3$ chimera compared to $\alpha 6/3$ and $\beta 2$ alone (data not shown).

The data in Figure 8 suggest that the $\beta 3$ subunit imparts some resistance to inhibition by TMPH and also that the extracellular domain of $\alpha 6$ has relatively little effect. We therefore tested oocytes expressing the complete wild-type $\alpha 6$ subunit. The $\alpha 6$ subunit was co-expressed with $\beta 4$ and $\beta 3$ since this is the only $\alpha 6$ combination we have found to work with any consistency in our hands. For these experiments, as a control we compared the oocytes injected with $\alpha 6\beta 4\beta 3$ to oocytes injected with $\alpha 3\beta 4\beta 3$. As shown in Figure 9, the oocytes expressing $\alpha 6\beta 4\beta 3$ showed relatively weak inhibition by TMPH during the co-application of TMPH and ACh, with an IC_{50} for the inhibition of net charge nearly an order of magnitude higher than for any other receptor subunit combination tested (Table 1). This reduced sensitivity to TMPH was most likely due to both the $\alpha 6$ and the $\beta 3$ subunits since $\alpha 3\beta 4\beta 3$ injected oocytes were much less sensitive than those expressing $\alpha 3\beta 4$ alone.

The responses of oocytes expressing $\alpha 6\beta 4\beta 3$ showed essentially full recovery after only a single wash period (Figure 9B). However, as with the oocytes expressing $\alpha 3$, $\beta 2$, and $\beta 3$, it is likely that the cells injected with $\alpha 3$, $\beta 4$, and $\beta 3$ had a mixed population of receptors since the recovery data was best fit with a two site model (Figure 9A).

Sequence in the pore-forming TM2 domain regulates TMPH inhibition.

While receptors containing pair-wise combinations with either $\beta 2$ or $\beta 4$ showed nearly irreversible inhibition by TMPH, inclusion of any of the common ancillary subunits ($\alpha 5$, $\alpha 6$ or $\beta 3$) resulted in more readily reversible inhibition. Sequence in the pore-forming second transmembrane domain (TM2) is important for regulating sensitivity to other non-competitive inhibitors, including mecamylamine and BTMPS, which is structurally-related to TMPH (Francis et al., 1998; Webster et al., 1999). As shown in Figure 10A, one point of sequence difference which stands out between $\beta 2$ and $\beta 4$ compared to the other neuronal nAChR is at the 10' position (i.e. the 10th residue within the second putative transmembrane domain (Miller, 1989)). Specifically, there is an alanine in $\beta 2$ and $\beta 4$ at this site and either a serine or threonine in subunits associated with reduced sensitivity to TMPH.

We co-expressed $\alpha 3$ and a previously published $\beta 4$ mutant (Webster et al., 1999) that contains a threonine substitution at the 10' site. Although these receptors were strongly inhibited during a co-application of 100 μ M ACh and 30 μ M TMPH, there was significant recovery after a single 5 minute washout (Figure 10B). The $\alpha 3\beta 410'T$ receptors recovered from TMPH inhibition with an estimated time constants of 25 ± 3 minutes, while for $\alpha 3\beta 4$ wild-types the estimated time constant for recovery was 450 ± 50 minutes (Figure 10C, wild-type data from Figure 3 shown for comparison).

Selective inhibition by TMPH of mixed receptor responses

Oocytes injected with a combination of $\alpha 7$ RNA and $\alpha 3$ plus $\beta 4$ RNA show responses that exhibit both fast and slow components (Figure 11A), hypothetically representing two populations of receptors. When these receptors are expressed separately, $\alpha 7$ receptors show only transient block by TMPH, while $\alpha 3\beta 4$ receptors show prolonged blockade. When TMPH and

ACh are co-applied to an oocyte injected with all 3 subunits, the rapid component of the response, presumably corresponding to the $\alpha 7$ receptors is resistant, as can be seen after a 5 minute wash out. In contrast, most of the slow component of the mixed response was eliminated by the ACh/TMPH co-application.

Note that with a simple co-application protocol there is a large transient current evoked, which we would hypothesize to be, at least in part, due to activation of both $\alpha 7$ and non- $\alpha 7$ receptors prior to the use-dependent effects of TMPH. However, since $\alpha 7$ receptors activate on the leading edge of the solution exchange (Papke and Papke, 2002; Papke and Thinschmidt, 1998), when the TMPH concentration would still be relatively low, they would be somewhat protected from full TMPH inhibition during co-application. Therefore, we also tested an alternative protocol which pre-applied TMPH alone at 30 μ M before the co-application of 30 μ M TMPH and 1 mM ACh. With this protocol (Figure 11B), the response was very effectively inhibited during the ACh/TMPH coapplication. There was significant recovery after a five minute wash out, and the recovered response had the rapid kinetics of a pure $\alpha 7$ response, indicating prolonged inhibition of the $\alpha 3\beta 4$ receptors selectively.

Neurons in the rat septum vary in their nAChR expression in ways that are correlated to their physiological and neurotransmitter phenotypes. Septal neurons that have fast firing rates, likely to be GABAergic, often have both fast and slow components to their ACh-evoked responses, with the fast component blockable by MLA. (Henderson et al., 2005; Thinschmidt et al., 2004). Figure 11C shows the ACh-evoked response from a septal neuron recording in a fresh brain slice. The co-application of TMPH and ACh evoked a relatively small response, suggesting that TMPH was an effective inhibitor of the neuronal nAChR in this ex-vivo preparation. During the coapplication peaks were reduced to 17 ± 3 % of the original average response (n=2) and the net charge of the coapplication responses were likewise reduced to 15 ± 10 %. After 3 minutes of washout following the TMPH application there was a differential recovery of peak and net charge. Peaks amplitude had returned to $95\% \pm 1\%$ of the control

amplitude while there was still a $43 \pm 9\%$ inhibition of the net charge. As shown in the figure insert, most of that net charge was associated with the $\alpha 7$ -like component of the current.

Discussion

Our experiments show that TMPH is a potent noncompetitive antagonist of neuronal nAChR. Its properties are in many ways similar to its bis analog BTMPS (Papke, 1993), except that TMPH can produce both use-dependent and for some receptor subtypes (notably the abundant $\alpha 4\beta 2$ subtype), inhibition that does not require prior channel activation. Such use-independent inhibition, coupled with slow reversibility suggests that relatively low steady concentrations of TMPH could profoundly down regulate the function of sensitive nAChR subtypes of the brain, beyond the levels that might be achieved by activity-driven inhibition.

While experimental agonists and antagonists are the most basic tools of pharmacology, agents with known selectivity for specific receptor subtypes are markedly better tools for understanding the molecular substrates of brain function and potential therapeutic targets. TMPH may be just such a tool for helping us understand brain nicotine receptors. However, neither BTMPS nor the prototypical ganglionic blocker mecamylamine have been tested on the same array of defined subunit combinations as were used in the current study, so the challenge remains to better understand the activity of these inhibitors.

In recent years the nomenclature for brain nAChR has been changing in such a way as to reflect our acknowledged uncertainty about the exact subunit composition of brain nAChR. What were previously referred to as $\alpha 4\beta 2$ receptors are now often $\alpha 4\beta 2^*$ or even just $\alpha 4^*$ receptors (Tapper et al., 2004), where the asterisk indicates the uncertain presence or absence of such ancillary subunits which we show determine the reversibility of TMPH inhibition. The present studies show the potential utility of TMPH as an experimental tool which may allow us in some cases to remove the asterisk and in other cases confirm its appropriateness.

The data obtained with the $\beta 4$ 10' mutant points to the importance of the neuronal $\beta 2$ and $\beta 4$ subunit TM2 sequence for defining the specificity of ganglionic blockers, and suggests at

least some mechanistic similarities between TMPH inhibition and inhibition by mecamylamine (Webster et al., 1999). The apparent requirement for an alanine at that level of the pore suggests that a hydrophobic interaction may be the basis for long-lived inhibition by TMPH. While it is a pharmacological convenience to have ganglionic blocking drugs which selectively inhibit neuronal receptors based on the beta subunit sequence, presumably this crucial sequence element plays some important, albeit unknown, functional role *in vivo*. Moreover, just as this site makes a crucial distinction between ganglionic and muscle-type receptors, it seems likely that it is of functional importance for those nAChR of the brain which incorporate the serine-containing ancillary subunits.

Based on its selectivity for long lived inhibition of some nAChR subunit combinations and relative sparing of others, TMPH will be useful in sorting out the effects associated with complex receptor subtypes with *in vitro* preparations such as fresh brain slices (Figure 11C). It may also show selectivity for blocking effects of nicotine *in vivo* (Damaj and Papke, in submitted). TMPH may also be of interest from the perspective of therapeutics since nicotinic antagonists have been proposed to be possible adjunct therapies for both Tourette's syndrome (Sanberg et al., 1998) and smoking cessation (Rose et al., 1994). The prototypical antagonist mecamylamine was used for these initial studies and the characterization of selective antagonists such as TMPH may lead the way to the development of better therapies for these, and potentially other, neuropsychiatric indications based on a more limited profile of side effects. Although the sensitivity of $\alpha 3\beta 4$ receptors to TMPH might suggest a high liability for peripheral side effects, this may not be the case since $\alpha 5$ is likely to be present in ganglionic receptors (Vernallis et al., 1993).

In conclusion, the results we report suggest that drug therapies for the inhibition of CNS nicotinic receptors may be developed with greater selectivity than previously appreciated. While more selective antagonists such as MLA are known, these generally work poorly with systemic administration. In addition to the potential therapeutic significance of TMPH, this drug may also

MOL (011676)

Selective inhibition of nAChR

prove to be a valuable tool to combine with selective agonists and knockout animals to further unravel the mystery of how neuronal nicotinic receptors play a role in brain function.

Acknowledgements:

We thank Julia Porter Papke for her technical assistance. We are very grateful to Axon Instruments for the use of an OpusXpress 6000A and pClamp9. We particularly thank Dr. Cathy Smith-Maxwell for her support and help with OpusXpress.

References

- Champtiaux N, Gotti C, Cordero-Erausquin M, David DJ, Przybylski C, Lena C, Clementi F, Moretti M, Rossi FM, Le Novere N, McIntosh JM, Gardier AM and Changeux JP (2003) Subunit composition of functional nicotinic receptors in dopaminergic neurons investigated with knock-out mice. *J Neurosci* **23**:7820-9.
- Dowell C, Olivera BM, Garrett JE, Staheli ST, Watkins M, Kuryatov A, Yoshikami D, Lindstrom JM and McIntosh JM (2003) Alpha-conotoxin PIA is selective for alpha6 subunit-containing nicotinic acetylcholine receptors. *J Neurosci* **23**:8445-52.
- Francis MM, Choi KI, Horenstein BA and Papke RL (1998) Sensitivity to voltage-independent inhibition determined by pore-lining region of ACh receptor. *Biophys. J.* **74**:2306-2317.
- Gerzanich V, Wang F, Kuryatov A and Lindstrom J (1998) alpha 5 Subunit alters desensitization, pharmacology, Ca⁺⁺ permeability and Ca⁺⁺ modulation of human neuronal alpha 3 nicotinic receptors. *J. Pharmacol. Exp. Ther.* **286**:311-20.
- Henderson Z, Boros A, Janzso G, Westwood AJ, Monyer H and Halasy K (2005) Somato-dendritic nicotinic receptor responses recorded in vitro from the medial septal diagonal band complex of the rodent. *J Physiol* **562**:165-82.
- Kuryatov A, Olale F, Cooper J, Choi C and Lindstrom J (2000) Human alpha6 AChR subtypes: subunit composition, assembly, and pharmacological responses. *Neuropharmacology* **39**:2570-90.
- Martin BR, Martin TJ, Fan F and Damaj MI (1993) Central actions of nicotine antagonists. *Med. Chem. Res.* **2**:564-577.
- Miller C (1989) Genetic manipulation of ion channels: a new approach to structure and mechanism. *Neuron* **2**:1195-205.
- Papke RL (1993) Use-dependent inhibition of neuronal nicotinic ACHR by Tinuvin® 770 (BIS (2, 2, 6, 6, - Tetramethyl-4-Piperidiny) Sebacacate), a possible additive to laboratory plastics, in *Biophy. J.* pp W-pos421.
- Papke RL and Papke JKP (2002) Comparative pharmacology of rat and human alpha7 nAChR conducted with net charge analysis. *Br J of Pharmacol* **137**:49-61.
- Papke RL, Sanberg PR and Shytle RD (2001) Analysis of mecamlamine stereoisomers on human nicotinic receptor subtypes. *J Pharmacol Exp Ther* **297**:646-56.
- Papke RL and Thinschmidt JS (1998) The Correction of Alpha7 Nicotinic Acetylcholine Receptor Concentration-Response Relationships in *Xenopus* Oocytes. *Neurosci. Let.* **256**:163-166.
- Rose JE, Behm FM, Westman EC, Levin ED, Stein RM and Ripka GV (1994) Mecamlamine combined with nicotine skin patch facilitates smoking cessation beyond nicotine patch treatment alone. *Clin. Pharmacol. Ther.* **56**:86-99.
- Sanberg PR, Shytle RD and Silver AA (1998) Treatment of Tourette's syndrome with mecamlamine. *Lancet* **352**:705-706.
- Tapper AR, McKinney SL, Nashmi R, Schwarz J, Deshpande P, Labarca C, Whiteaker P, Marks MJ, Collins AC and Lester HA (2004) Nicotine activation of alpha4* receptors: sufficient for reward, tolerance, and sensitization. *Science* **306**:1029-32.
- Thinschmidt JS, King MA, Frazier CJ, Meyer EM and Papke RL (2004) Medial Septum/Diagonal Band Cells Express Multiple Functional Nicotinic Receptor Sub-Types That Are Correlated With Firing Frequency. *34th Annual Meeting of the Society for Neuroscience* **842**:15.

- Vernallis AB, Conroy WG and Berg DK (1993) Neurons assemble acetylcholine receptors with as many as three kinds of subunits while maintaining subunit segregation among receptor subtypes. *Neuron* **10**:451-464.
- Wang F, Gerzanich V, Wells GB, Anand R, Peng X, Keyser K and Lindstrom J (1996) Assembly of Human Neuronal Nicotinic Receptor $\alpha 5$ Subunits with $\alpha 3$, $\beta 2$ and $\beta 4$ Subunits. *J. Biol. Chem.* **271**:17656-65.
- Webster JC, Francis MM, Porter JK, Robinson G, Stokes C, Horenstein B and Papke RL (1999) Antagonist activities of mecamylamine and nicotine show reciprocal dependence on beta subunit sequence in the second transmembrane domain. *Br. J. Pharmacol.* **127**:1337-48.

MOL (011676)

Selective inhibition of nAChR

Footnotes:

This work was supported by National Institute on Drug Abuse grant DA 017548, NIH grants NS 32888, PO1 AG10485 and MH 11258 and the University of Florida College Incentive fund.

Figure legends

Figure 1. TMPH produces selective long-term inhibition of neuronal ganglionic type $\alpha 3\beta 4$ receptors. **A)** The chemical structure of TMPH. **B)** The upper panel shows raw data traces obtained from an oocyte expressing mouse muscle-type $\alpha 1\beta 1\epsilon\delta$ subunits to the application of either 10 μM ACh alone (open circles) or the co-application of 10 μM ACh and 300 nM TMPH (arrow). The lower panel is the averaged normalized data (\pm SEM, $n \geq 4$) from oocytes expressing $\alpha 1\beta 1\epsilon\delta$ subunits to the co-application 10 μM ACh and a range of TMPH concentrations. **C)** The upper panel shows raw data traces obtained from an oocyte expressing rat ganglionic-type $\alpha 3\beta 4$ subunits to the application of either 100 μM ACh alone (open circles) or the co-application of 100 μM ACh and 300 nM TMPH (arrow). The lower panel is the averaged normalized data (\pm SEM, $n \geq 4$) from oocytes expressing $\alpha 3\beta 4$ subunits to the co-application 100 μM ACh and a range of TMPH concentrations. Three values are plotted in each of the concentration-response curves: (\blacklozenge) the peak current amplitude of the co-application response, normalized to the peak amplitude of the previous ACh control; (\blacktriangledown) the net charge of the co-application response, normalized to the net charge of the previous ACh control (Papke and Papke, 2002); and (\bullet) the peak current amplitude of the ACh control response obtained after the TMPH/ACh co-application, normalized to the peak amplitude of the previous ACh control.

Figure 2. TMPH inhibition of responses obtained from oocytes expressing rat neuronal nAChR subunits. Shown are the averaged normalized data (\pm SEM, $n \geq 4$) from oocytes expressing $\alpha 4\beta 2$, $\alpha 3\beta 2$, and $\alpha 7$ subunits (from top to bottom respectively) to the co-application ACh and a range of TMPH concentrations. Three values are plotted in each of the concentration-response curves: (\blacklozenge) the peak current amplitude of the co-application response, normalized to the peak amplitude of the previous ACh

control; (▼) the net charge of the co-application response, normalized to the net charge of the previous ACh control; and (●) the peak current amplitude of the ACh control response obtained after the TMPH/ACh co-application, normalized to the peak amplitude of the previous ACh control. The control ACh concentrations used were 10 μ M, 30 μ M, and 300 μ M for α 4 β 2, α 3 β 2, and α 7, respectively.

Figure 3. TMPH produces long-term inhibition of neuronal beta subunit-containing nAChR but not α 7 homomeric receptors. ACh and TMPH were co-applied at time 0 to oocytes expressing rat α 3 β 4, α 4 β 2, α 3 β 2, or α 7 subunits. Subsequently, control ACh applications were made at 5 min intervals to measure recovery. The control ACh concentrations used were 100 μ M, 10 μ M, 30 μ M, and 300 μ M for α 3 β 4, α 4 β 2, α 3 β 2, and α 7, respectively. The initial inhibition was produced by the co-application of ACh at the control concentration and 30 μ M TMPH, except in the case of the α 3 β 2 receptors, which were inhibited by the co-application of ACh and 3 μ M TMPH.

Figure 4. Varying amounts of use-independent inhibition of neuronal beta subunit-containing receptors by TMPH. **A)** Representative data showing the effects of the application of 1 μ M TMPH alone to α 4 β 2 and α 3 β 2 expressing oocytes (open arrows), compared to the application of to ACh alone (open circles) either before or after the application of TMPH. The control ACh concentrations used were 10 μ M and 30 μ M for α 4 β 2 and α 3 β 2, respectively. **B)** Comparison of the use-dependent (1 μ M TMPH + ACh) and use-independent (1 μ M TMPH alone) inhibition of α 3 β 4, α 4 β 2, and α 3 β 2 receptors by TMPH. The data are calculated from the peak amplitudes of control ACh responses obtained after the application of TMPH \pm ACh, expressed relative to the peak current amplitude of ACh control responses prior to the application of TMPH.

Figure 5. Cumulative inhibition by repeated application of TMPH. **A)** Responses of an oocyte expressing $\alpha 4\beta 2$ receptors to alternating applications of 30 μM ACh alone (open circles) or 30 μM ACh plus 100 nM TMPH (arrows). The total inhibition increased during the first 3 TMPH/ACh co-applications. Note that the TMPH/ACh co-applications differ in kinetics from the ACh controls, showing a greater inhibition of net charge than of peak current. **B)** Normalized average responses of oocytes expressing $\alpha 4\beta 2$ receptors ($\pm\text{SEM}$, $n \geq 4$) to alternating applications of ACh alone or ACh plus TMPH, as in panel A. Both peak currents and net charge values are plotted, normalized to the ACh control response recorded before the first ACh/TMPH co-application ($t = -5$ minutes). Note that the traces in panel A are shown on the same time scale as the X-axis in panel B.

Figure 6 TMPH inhibition of responses obtained from oocytes expressing human neuronal nAChR subunits. Shown are the averaged normalized data ($\pm\text{SEM}$, $n \geq 4$) from oocytes expressing human $\alpha 3\beta 2$ or $\alpha 3\beta 2\alpha 5$ subunits (top and bottom, respectively) to the co-application ACh and a range of TMPH concentrations. Three values are plotted in each of the concentration-response curves: (\blacklozenge) the peak current amplitude of the co-application response, normalized to the peak amplitude of the previous ACh control; (\blacktriangledown) the net charge of the co-application response, normalized to the net charge of the previous ACh control; and (\bullet) the peak current amplitude of the ACh control response obtained after the TMPH/ACh co-application, normalized to the peak amplitude of the previous ACh control. The control ACh concentrations used were 30 μM and 1 μM for $\alpha 3\beta 2$ and $\alpha 3\beta 2\alpha 5$ expressing oocytes, respectively.

Figure 7 The recovery of human $\alpha 5$ -containing $\alpha 3\beta 2$ receptors from TMPH-produced inhibition is rapid compared to the recovery of receptors formed with $\alpha 3\beta 2$ subunits alone. **A)** Representative traces obtained from oocytes expressing human $\alpha 3\beta 2$ or $\alpha 3\beta 2\alpha 5$ subunits. Following an initial application of ACh alone (open circle), a single co-application was made of ACh and 1 μM TMPH (arrow). Recovery was evaluated by making repeated control ACh applications at 5 minute intervals (open circles). **B)** Normalized average responses of oocytes expressing $\alpha 3\beta 2$ or $\alpha 3\beta 2\alpha 5$ receptors ($\pm\text{SEM}$, $n \geq 4$) to repeated applications of ACh alone, following a single application of ACh plus TMPH (as in panel A). Peak currents are plotted, normalized to the ACh control response recorded before the ACh/TMPH co-application. Note that the traces in panel A are shown on the same time scale as the X-axis in panel B.

Figure 8. TMPH inhibition of responses obtained from oocytes expressing $\beta 3$ and chimeric $\alpha 6/\alpha 3$ subunits. Shown are the averaged normalized data ($\pm\text{SEM}$, $n \geq 4$) from oocytes expressing human $\alpha 3\beta 2\beta 3$ or $\alpha 6/3\beta 2\beta 3$ subunits (top and bottom, respectively) to the co-application ACh and a range of TMPH concentrations. Three values are plotted in each of the concentration-response curves: (\blacklozenge) the peak current amplitude of the co-application response, normalized to the peak amplitude of the previous ACh control; (\blacktriangledown) the net charge of the co-application response, normalized to the net charge of the previous ACh control; and (\bullet) the peak current amplitude of the ACh control response obtained after the TMPH/ACh co-application, normalized to the peak amplitude of the previous ACh control. The control ACh concentration used was 100 μM .

Figure 9. TMPH inhibition of responses obtained from oocytes expressing b4, $\beta 3$ and either $\alpha 3$ (A) or $\alpha 6$ subunits (B). Shown are the averaged normalized data ($\pm\text{SEM}$, $n \geq 4$) to the co-application 100 μM ACh and a range of TMPH concentrations. Three

values are plotted in each of the concentration-response curves: (◆) the peak current amplitude of the co-application response, normalized to the peak amplitude of the previous ACh control; (▼) the net charge of the co-application response, normalized to the net charge of the previous ACh control; and (●) the peak current amplitude of the ACh control response obtained after the TMPH/ACh co-application, normalized to the peak amplitude of the previous ACh control. Note that the recovery data for oocytes expressing $\alpha 3$, $\beta 4$, and $\beta 3$ could not be fit to a one site model. The curve fit show is for a 2 site model with approximately 15% fit to an IC_{50} of 1 μM and 85% fit to an IC_{50} of 30 μM .

Figure 10. Amino acid sequence in the pore-forming transmembrane domain regulates TMPH inhibition. **A)** Sequence of TM2 domains of the nAChR subunits in this study. The sequences are aligned and numbered as proposed by Miller (1989). The 10' site is highlighted. **B)** Representative responses of an oocyte co-expressing $\alpha 3$ and a $\beta 4$ mutant in which a threonine was substituted for the alanine at the 10' position. Shown are responses to 100 μM ACh alone, 100 μM ACh co-applied with 30 μM TMPH, and again 100 μM ACh alone. Responses were recorded from the same oocyte at 5 minute intervals. During the co-application, peak currents were reduced on average ($n = 8$) to 9.8 ± 1.0 % of the control and the net charge during the co-application was reduced to 7.7 ± 1.2 % of the controls. **C)** Progressive recovery of oocytes expressing $\alpha 3$ and the $\beta 4$ 10'T mutant. Data at $t=0$ represents the average inhibition of peak currents during the co-application of ACh and TMPH. Following points represent the responses to subsequent applications of ACh alone at 5 minute intervals. Points represent the average ($\pm SEM$) of at least 4 oocytes and the data were normalized to the peak responses obtains 5 minutes prior to the ACh/TMPH co-application. Data for the $\alpha 3\beta 4$ wild type (from Figure 3) are provided for

comparison. Time constants were estimated from exponential functions fit to the data (not shown).

Figure 11. Long-term inhibition of the slow components of mixed nicotinic receptor mediated responses. **A)** Responses of an oocyte injected with RNA coding for $\alpha 7$ as well as $\alpha 3$ and $\beta 4$. The first response was evoked by the application of 1 mM ACh (solid bar). The second response was evoked by the application of 1 mM ACh plus 30 μ M TMPH (open bar). The subsequent responses shown were to additional applications of 1 mM ACh alone at 5 minute intervals. The expanded traces below show the two kinetic components in the ACh-evoked responses prior to (*) and following (**) the TMPH/ACh co-application. In the traces on the left, an estimate of the slow component is shaded out, to illustrate the relative sparing of the fast $\alpha 7$ -like component. **B)** Shown are the responses of an oocyte expressing both $\alpha 3\beta 4$ and $\alpha 7$ -type receptors. Before the co-application-evoked response 30 μ M TMPH was preapplied for 30 s in order to assure that the full concentration of TMPH was present during the early $\alpha 7$ -mediated phase of the mixed receptor response. Even though transient inhibition was increased with this protocol compared to the simple preapplication protocol shown in A, there was good recovery of a fast component of the mixed response after only a 5 minute wash. **C)** Responses from a patch-clamped neuron in a rat brain slice of the septum. A double-barreled pico-spritzer pressure application system was used with one barrel containing 1 mM ACh and the other containing 1 mM ACh and 300 μ M TMPH. Three initial responses to ACh alone were obtained at 30 s intervals and the averaged response is shown (*). Two applications separated by 30 s were then made from the barrel containing both TMPH and ACh and the average of those responses is shown. After the ACh/TMP applications, ACh alone was repeatedly applied at 30 s intervals. Shown are the averages of 2 traces obtained after either 60 and 90 s washout or 150 and 180 s

washout (**). As shown in the overlay at the bottom, after washout the peak current amplitudes of the average response (gray) were essentially the same as the average response prior to the TMPH (black) application, but the late phase of the current is largely absent. Initial responses of the neuron to ACh (*) were well fit with 2-exponential decay rates, with 2 time constants of 218 and 12 ms representing 21 and 79% of the area respectively. After 2.5-3 minutes of recovery (**), the current decay was best fit with 2 time constants of 100 and 10 ms, representing 13 and 87% of the area, respectively.

Table 1: *In vitro* data.

	IC ₅₀ (peak)	IC ₅₀ (area)	IC ₅₀ (recovery)
Mouse Muscle	276 ± 20 nM	390 ± 50 nM	27 ± 5.5 μM
Rat α7	1.0 ± 0.1 μM	1.2 ± 0.2 μM	16 ± 4 μM
Rat α4β2	1.4 ± 0.3 μM	110 ± 40 nM	250 ± 80 nM
Rat α3β4	200 ± 50 nM	75 ± 23 nM	85 ± 32 nM
Rat α3β2	3.7 ± 1.2 μM	440 ± 90 nM	230 ± 30 nM
Human α3β2	3.7 ± 1.2 μM	460 ± 170 nM	400 ± 120 nM
Human α3β2α5	1.1 ± μM	430 ± 180 nM	750 ± 200 nM
Rat α3β2β3	120 ± 80 μM	2.7 ± 0.6 μM	4.3 ± 1.5 μM
Rat α6/3β2β3	60 ± 20 μM	1.0 ± 0.3 μM	2.3 ± 0.5 μM
Rat α3β4β3	1.9 ± 0.2 μM	1.4 ± 0.2 μM	30 ± 50 μM, 1.0 ± 0.6 μM*
Rat α6β4β3	11.0 ± 4.4μM	18.3 ± 4.9 μM	1700 ± 420 μM

IC₅₀ values were calculated based on either the decrease in peak current amplitudes or the decrease in the net charge of the ACh response when co-applied with TMPH. For many of the subunit combinations tested there was no detectable recovery after a 5 minute wash and so IC₅₀ values were also calculated based on the inhibition still present at the 5 minute time point (recovery). Note that these IC₅₀ values are based on standard single application protocol and are likely to underestimate the IC₅₀ for steady-state conditions.

MOL (011676)

Selective inhibition of nAChR

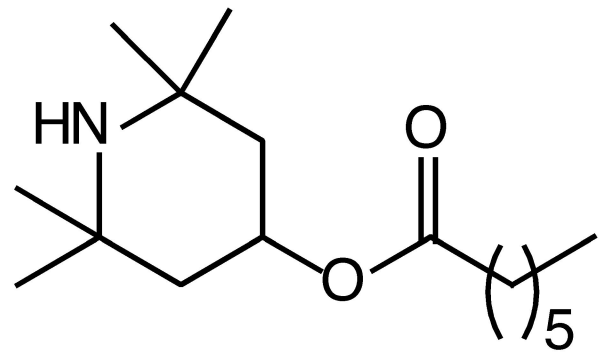
*The data for the recovery of cells expressing $\alpha 3\beta 4\beta 3$ were fit to a 2 site model (see Figure 9).

Table 2: *In vitro* data.

	IC ₅₀ net charge/ IC ₅₀ peak	IC ₅₀ recovery/ IC ₅₀ net charge
mouse $\alpha 1\beta 1\delta\epsilon$	1.4	69
rat $\alpha 7$	1.2	13.3
rat $\alpha 4\beta 2$	0.08	2.3
rat $\alpha 3\beta 4$	0.36	1.1
rat $\alpha 3\beta 2$	0.12	0.52
human $\alpha 3\beta 2$	0.12	0.87
human $\alpha 3\beta 2\alpha 5$	0.15	1.7
rat $\alpha 3\beta 2\beta 3$	0.025	1.6
rat $\alpha 6/3\beta 2\beta 3$.017	2.0
rat $\alpha 3\beta 4\beta 3$	0.74	0.7, 21*
rat $\alpha 6\beta 4\beta 3$	1.7	93

The value "IC₅₀ (recovery)" reflects the residual inhibition of the ACh control response measured after a 5 minute wash. If IC₅₀(recovery) > IC₅₀(area), then there was significant recovery (i.e. readily reversible inhibition). Likewise if IC₅₀(area) < IC₅₀(peak), then there was significant buildup of inhibition throughout the agonist/antagonist co-application.

*The data for the recovery of cells expressing $\alpha 3\beta 4\beta 3$ was fit to a 2 site model (see Figure 9).

A**TMPH**

2,2,6,6-tetramethylpiperidin-4-yl heptanoate

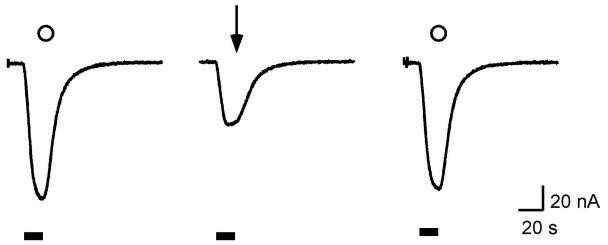
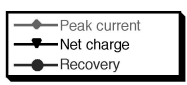
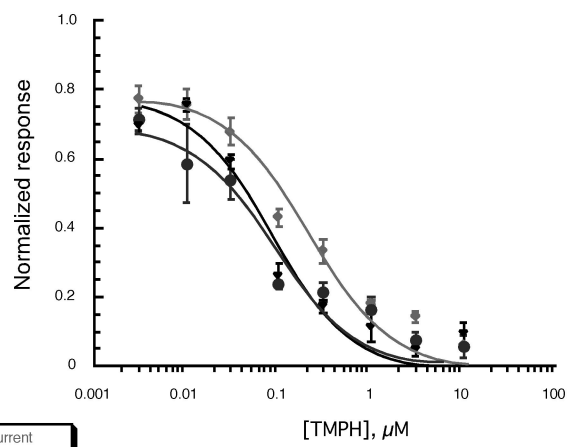
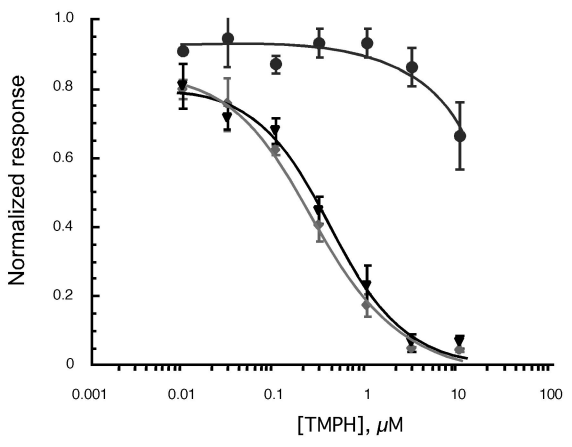
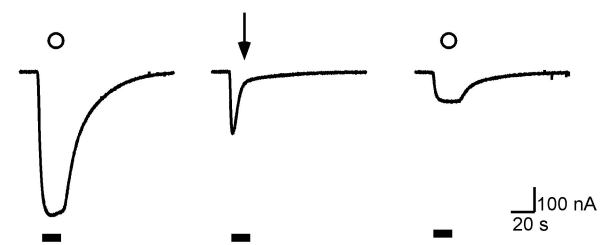
B $\alpha 1\beta 1\epsilon\delta$ **C** $\alpha 3\beta 4$ 

Figure 1

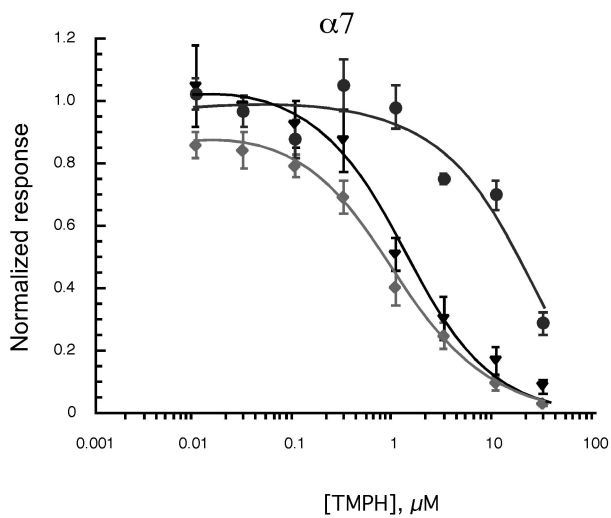
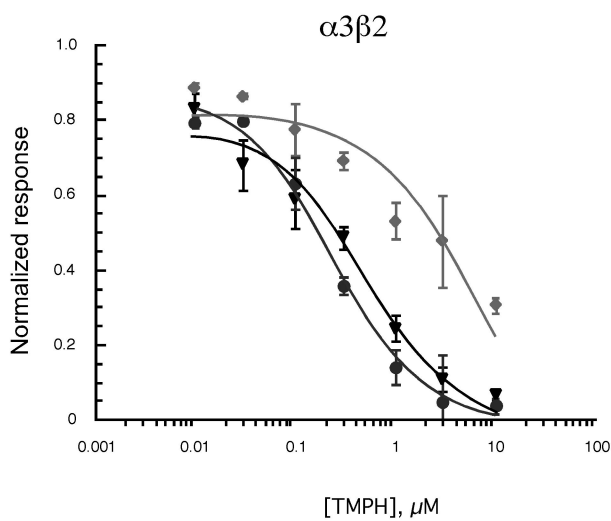
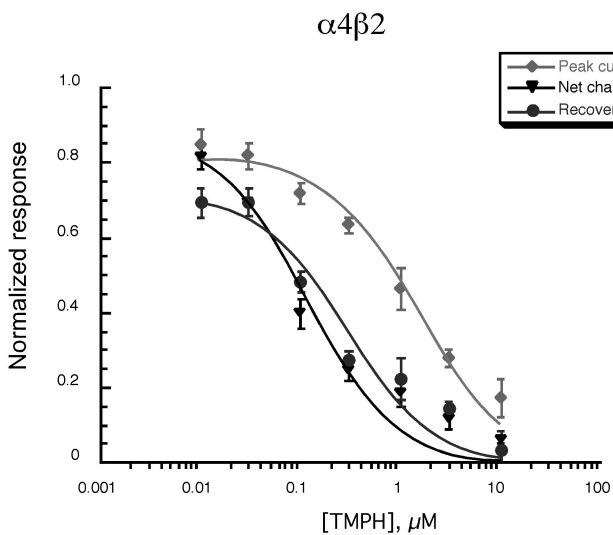


Figure 2

Rat neuronal nAChR

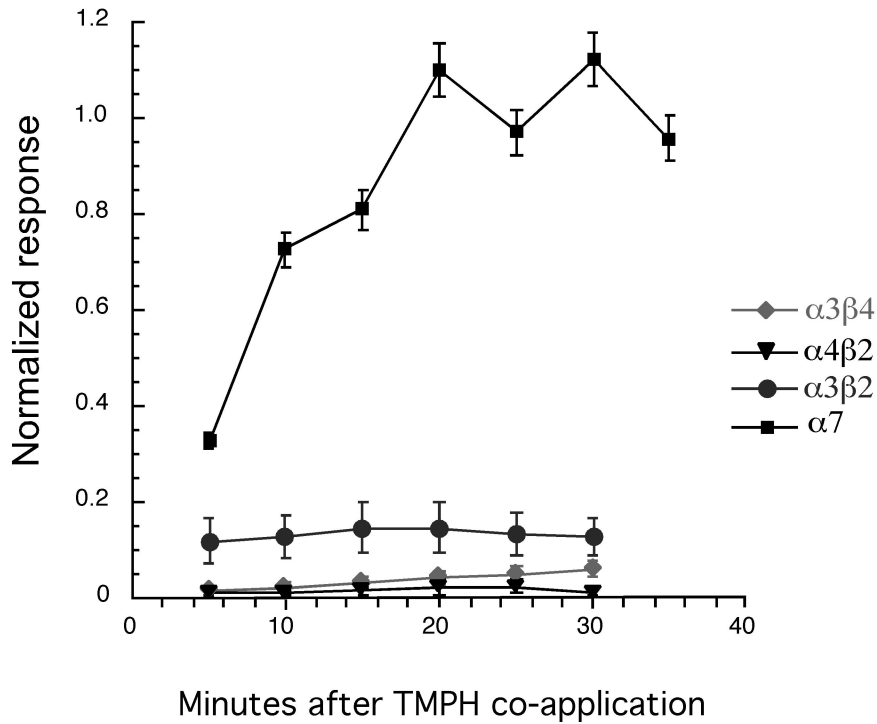


Figure 3

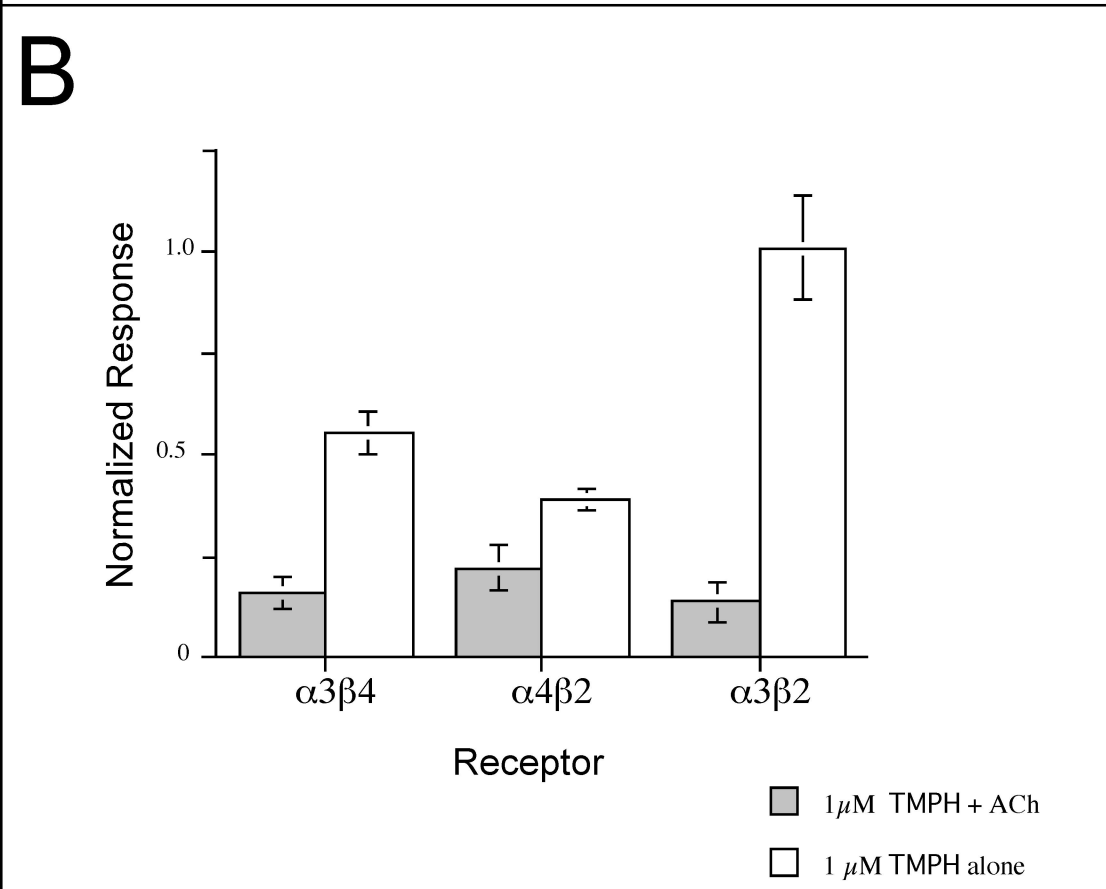
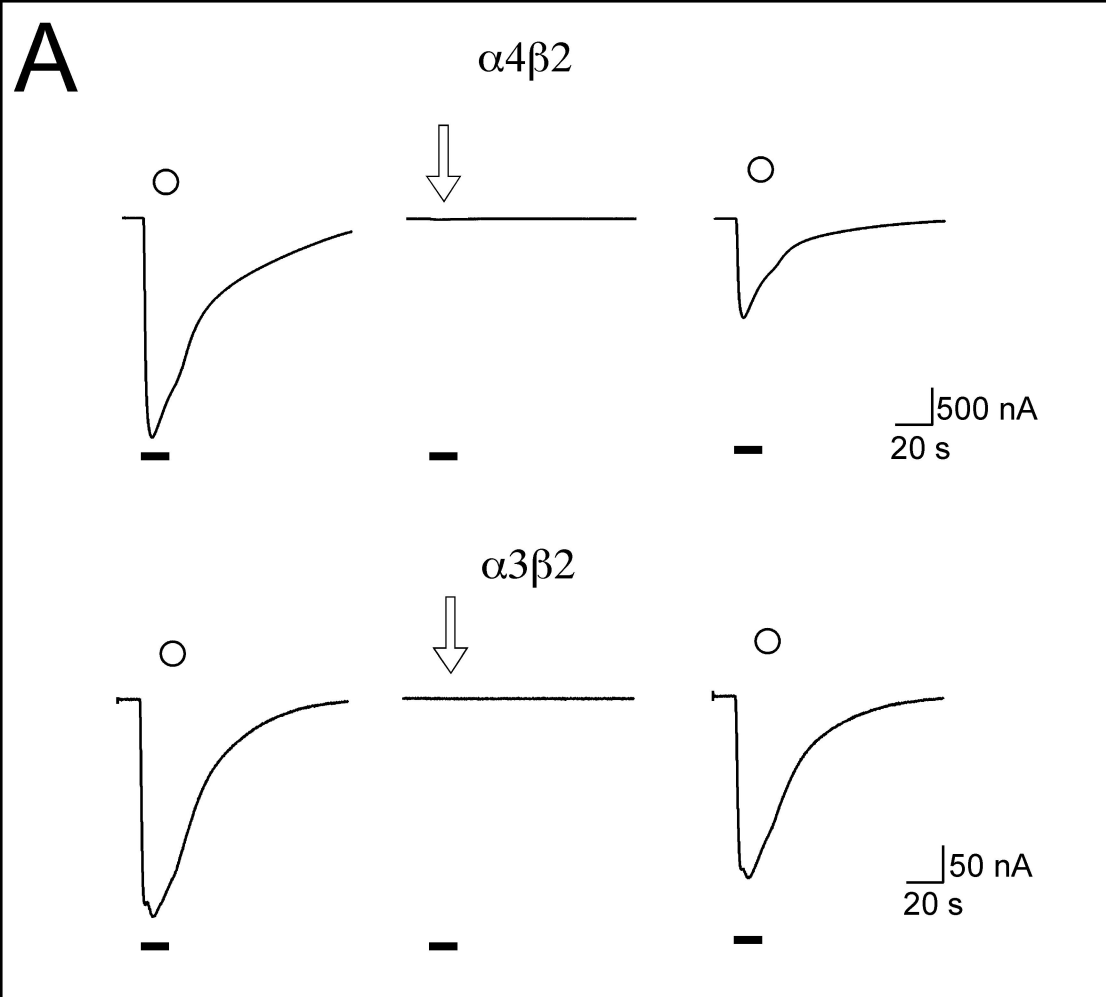


Figure 4

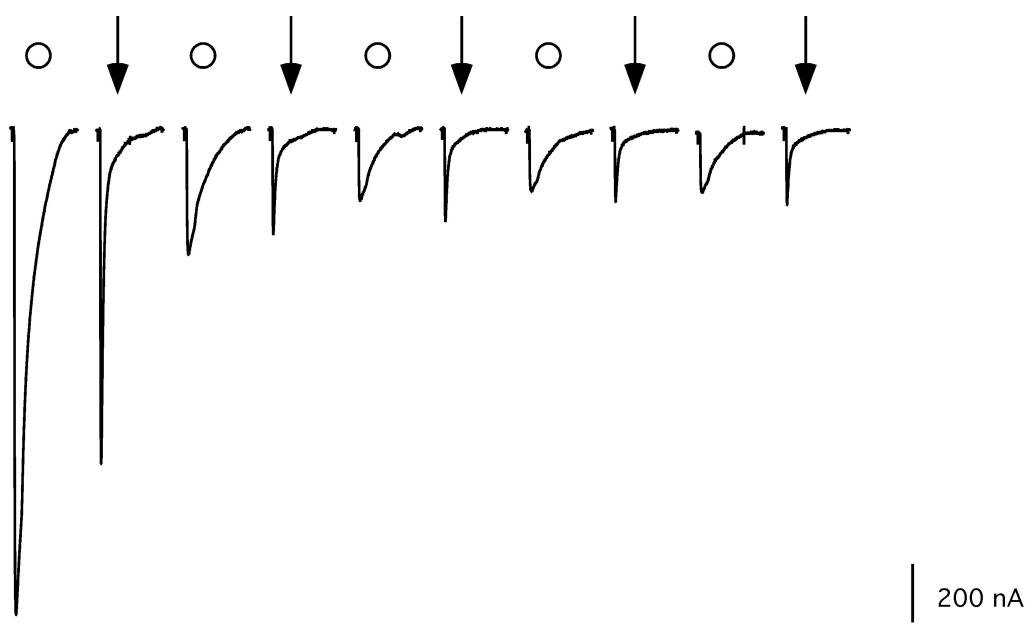
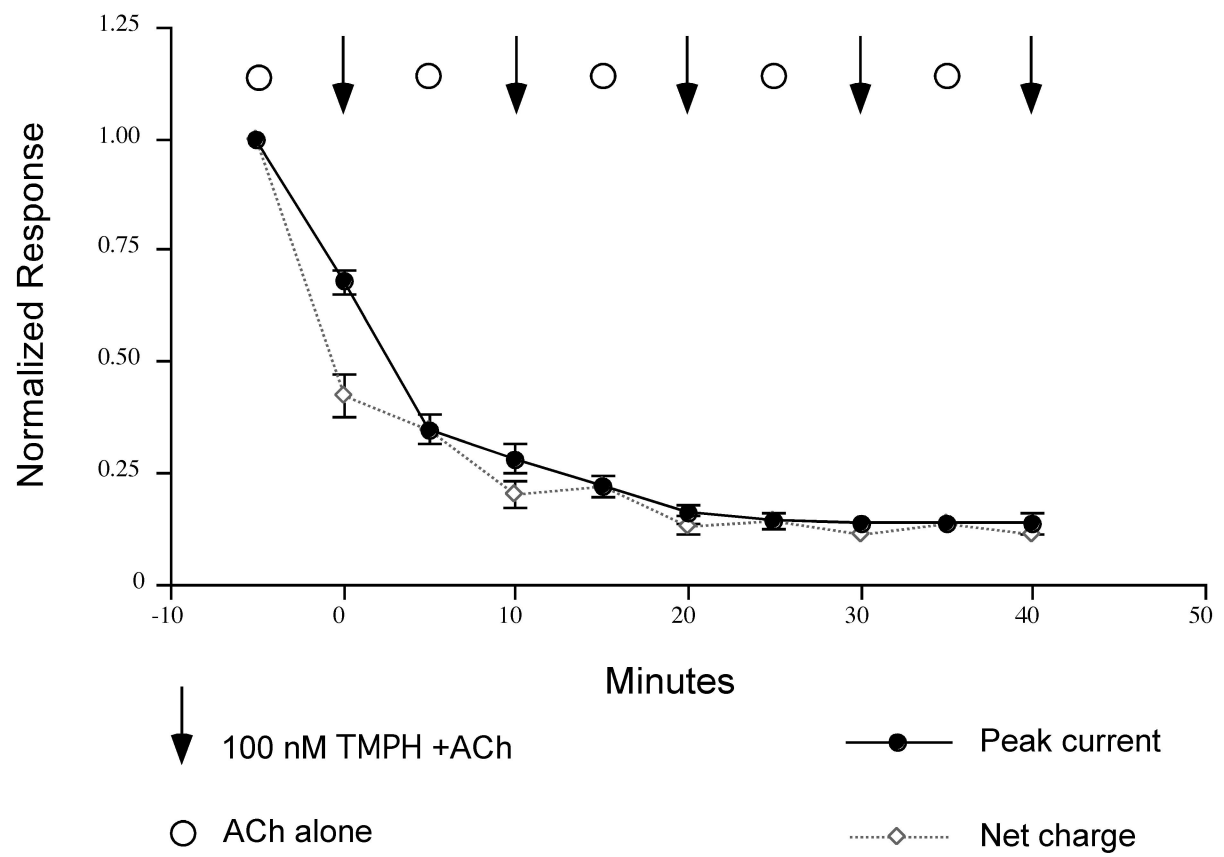
A**B**

Figure 5

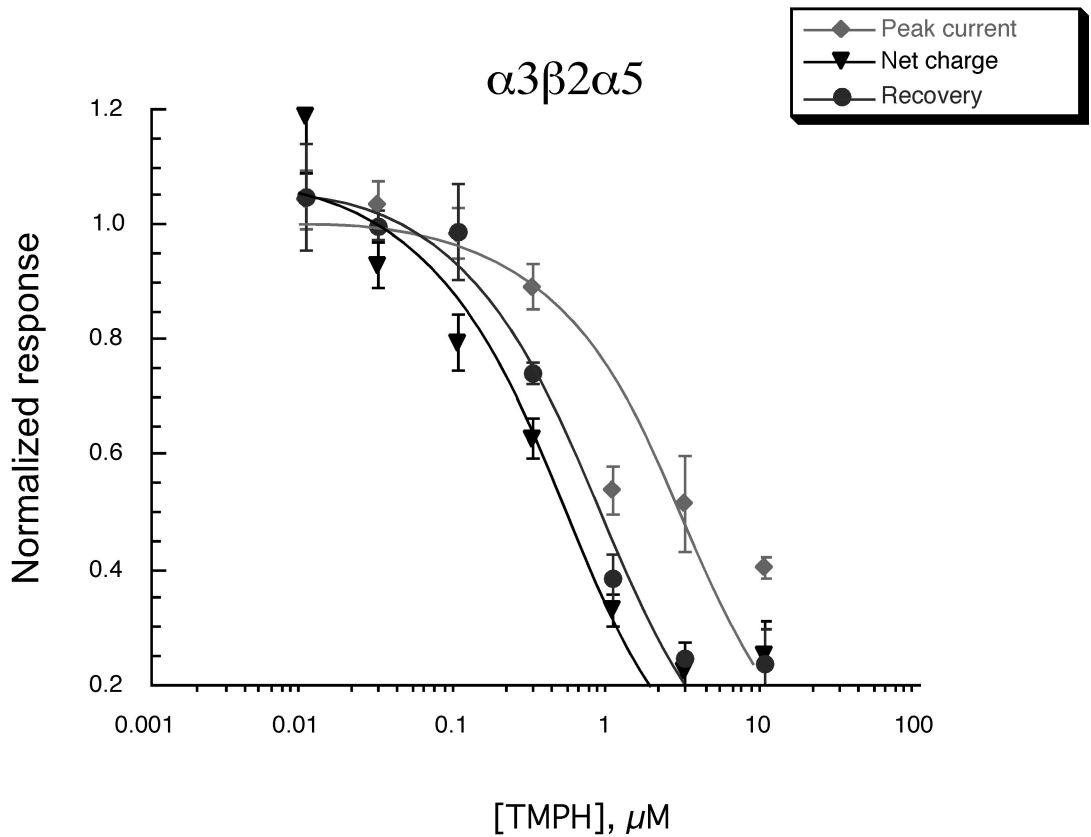
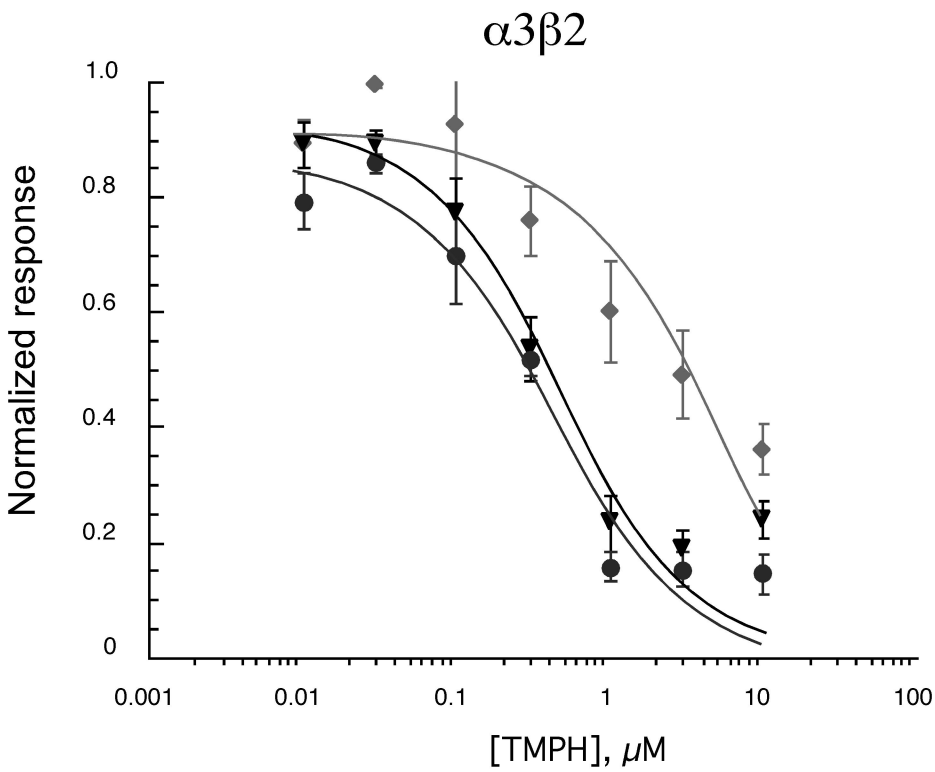


Figure 6

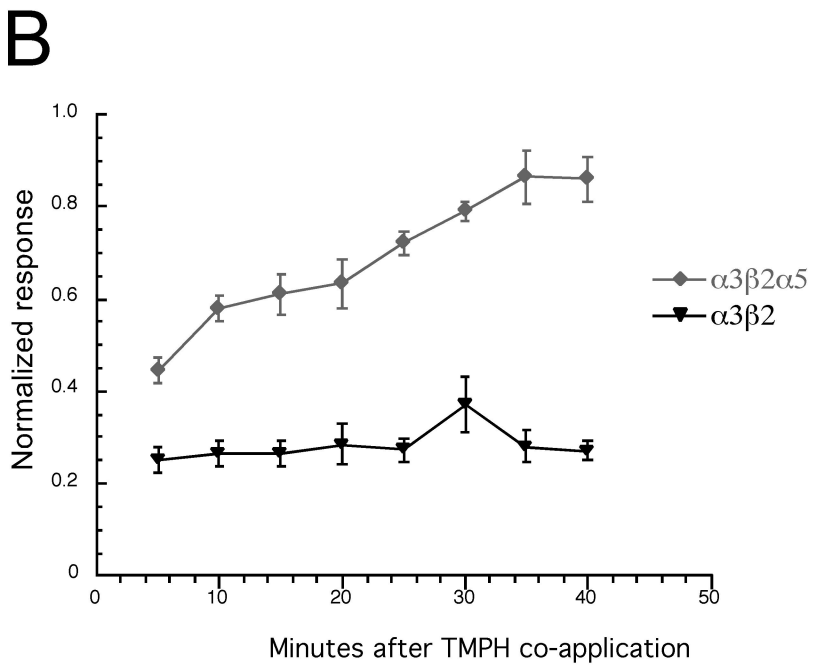
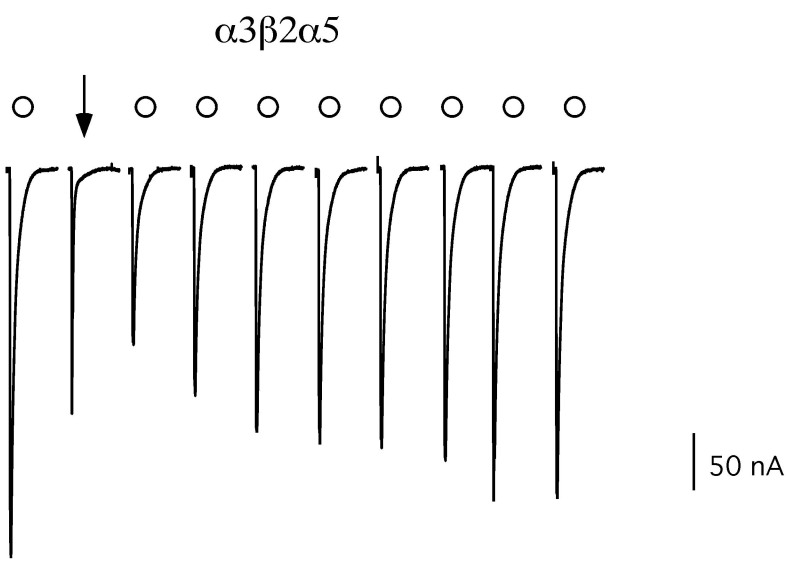
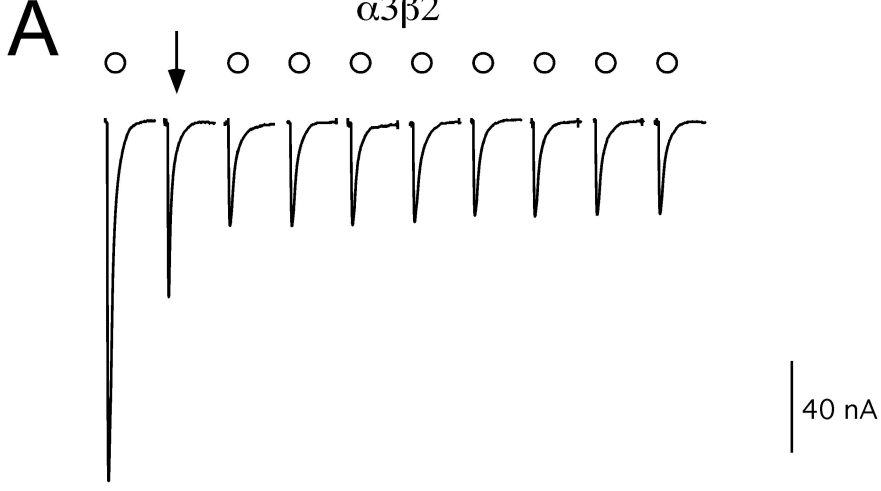


Figure 7

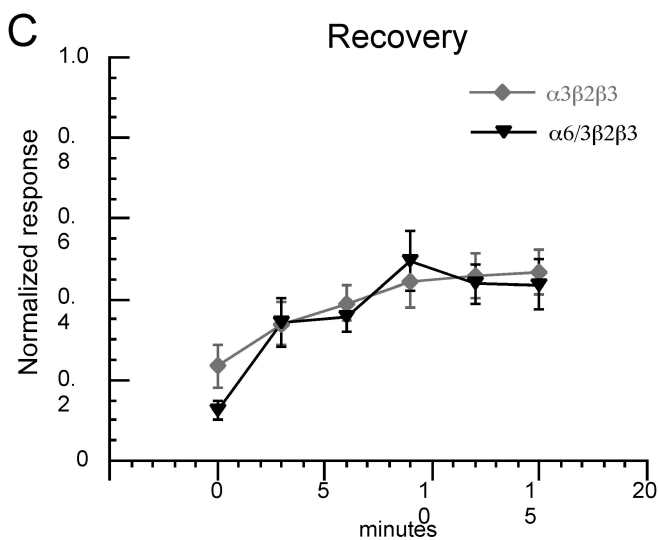
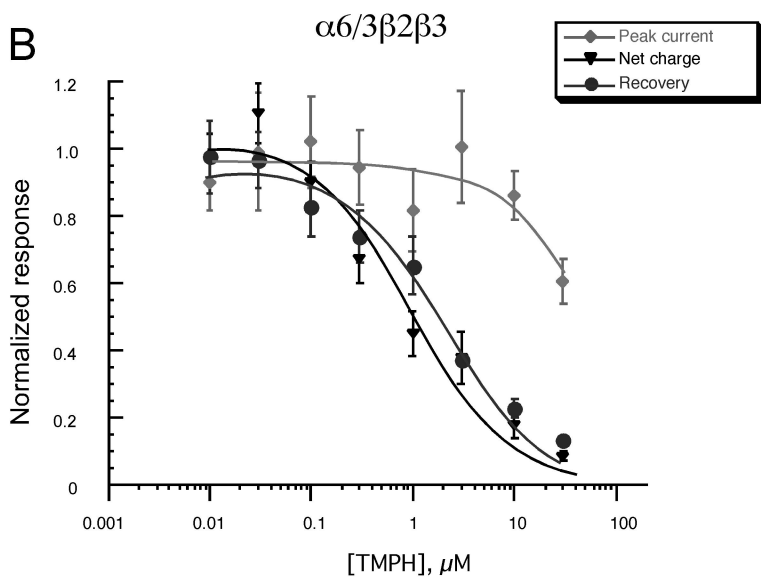
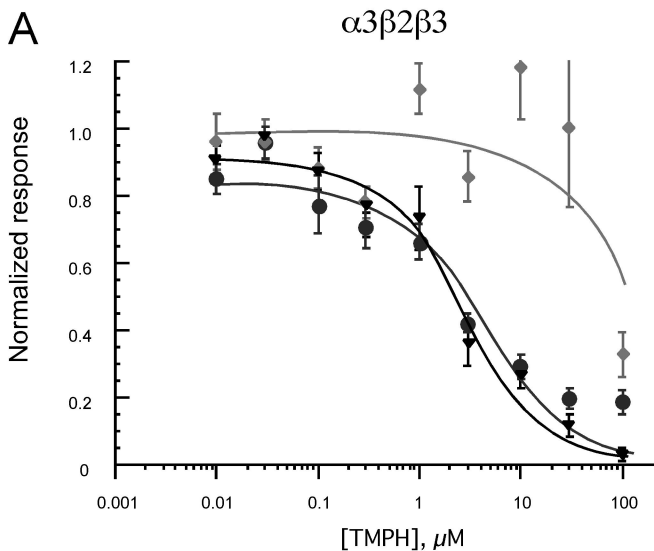


Figure 8

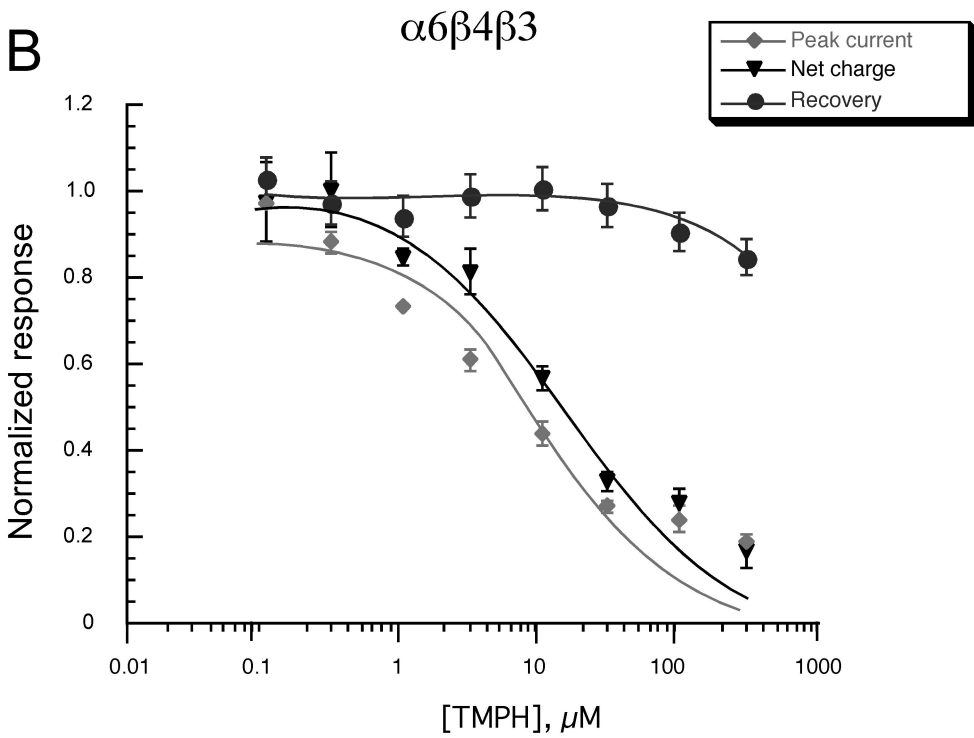
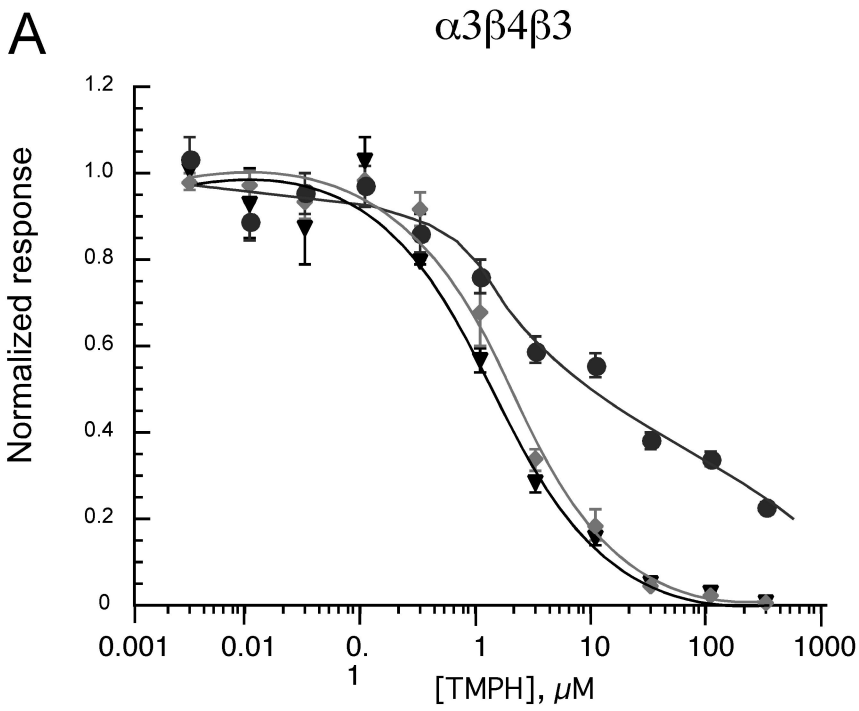


Figure 9

A

TM2 sequences

$\beta 4$	MTLCISVLLA	LTFFLLLLISK
$\beta 2$	MTLCISVLLA	LTVFLLLLISK
$\alpha 5$	ISLCTSVLV	SLTVFLLVIEE
$\alpha 6$	VTLCISVLLS	SLTVFLLVITE
$\beta 3$	LSLSTSVLV	SLTVFLLVIEE
$\alpha 7$	ISLGITVLLS	SLTVFMLLVAE
	1'	20'
$\alpha 4$	VTLCISVLLS	SLTVFLLLLITE
$\alpha 3$	VTLCISVLLS	SLTVFLLVITE
$\alpha 1$	MTLSISVLLS	SLTVFLLVIVE
$\beta 1$	MGLSIFALLT	SLTVFLLLLAD
ϵ	TSVAISVLLA	QSVFLLLLISK
δ	TSVAISVLLA	QSVFLLLLISK

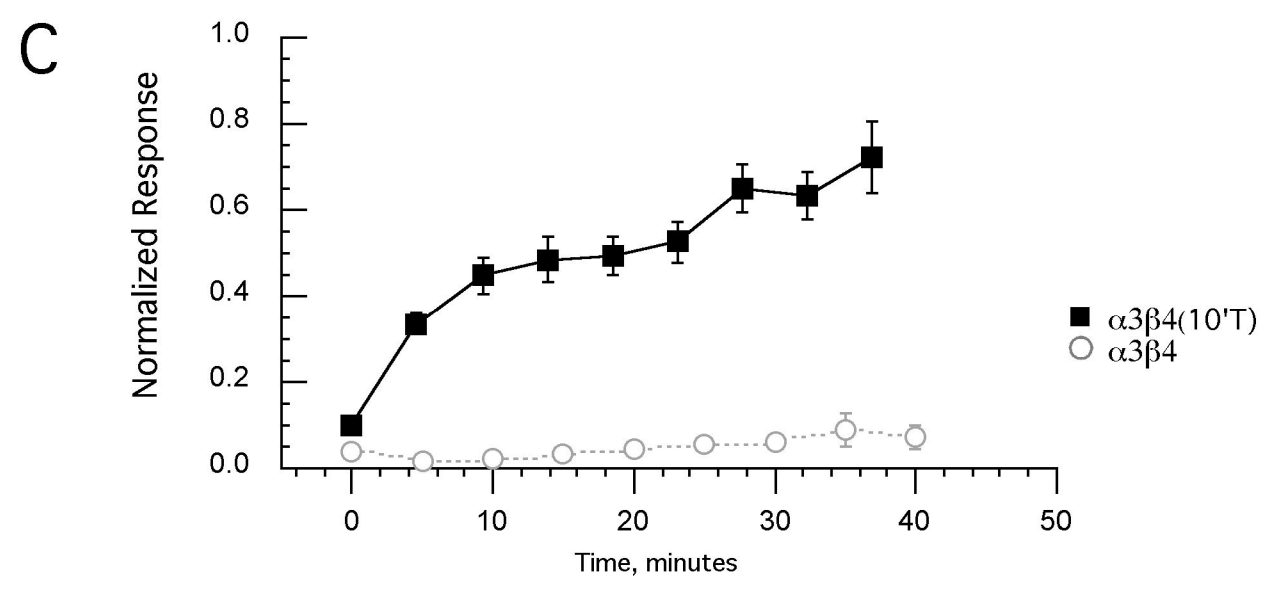
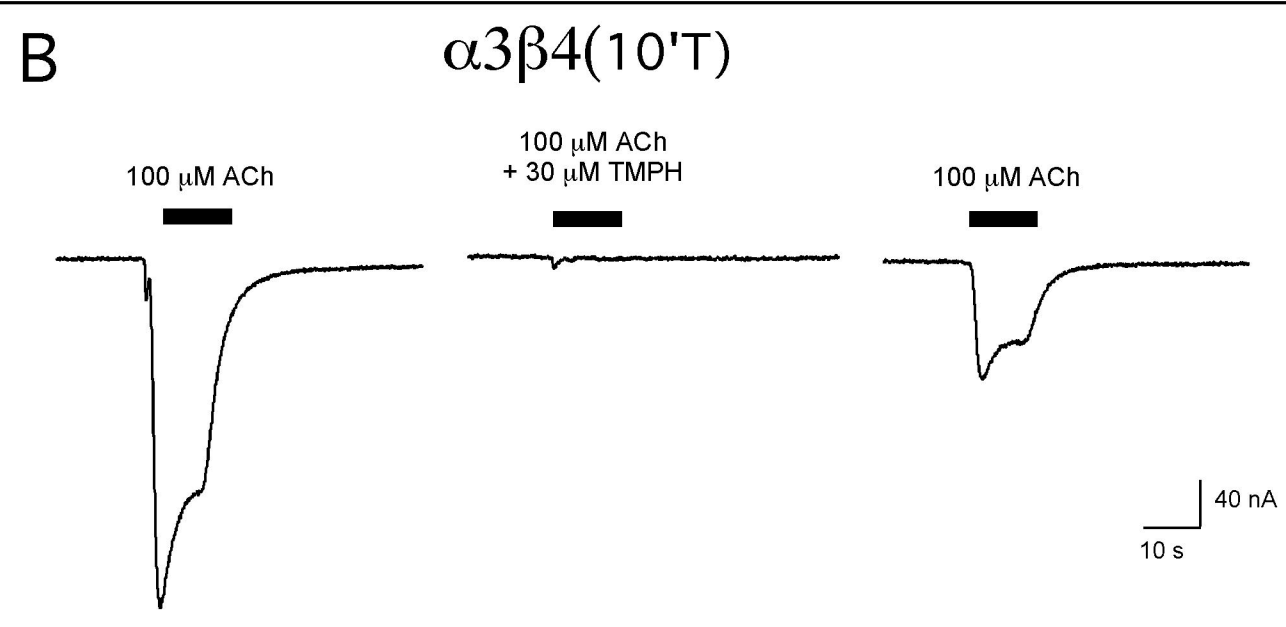


Figure 10

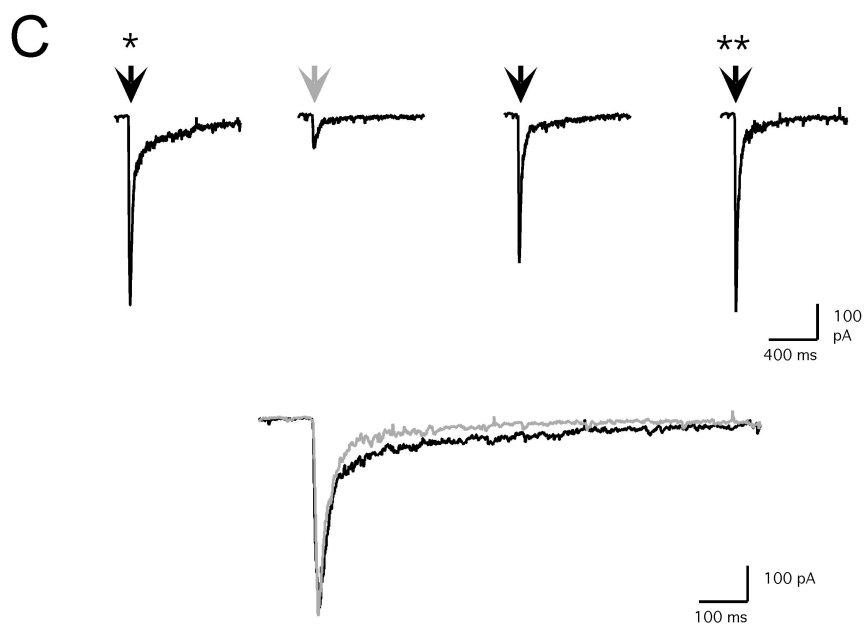
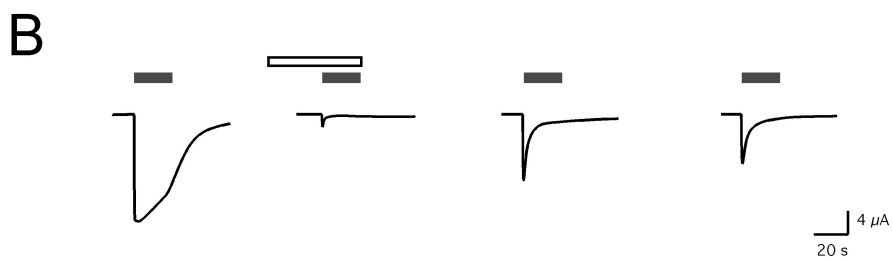
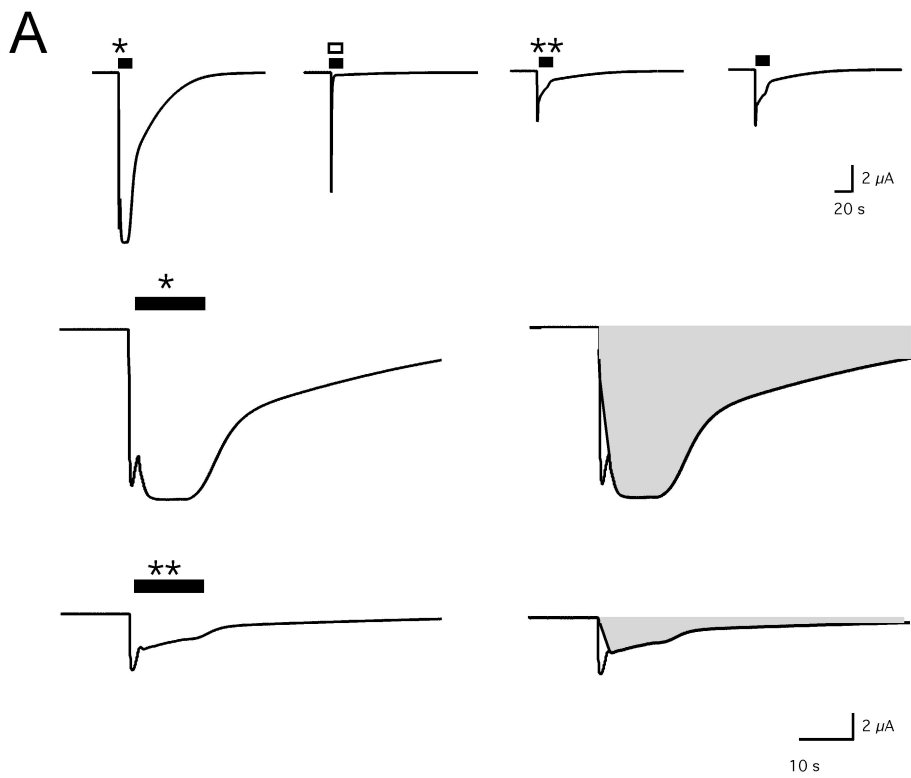


Figure 11